

## Visual fields of four batoid fishes: a comparative study

D. Michelle McComb\* and Stephen M. Kajiura

Biological Sciences, Florida Atlantic University, Boca Raton, FL 33431, USA

\*Author for correspondence (e-mail: dmccomb@fau.edu)

Accepted 12 December 2007

### SUMMARY

The visual fields of elasmobranch fishes are not well characterized even though this is a fundamental element of the visual system. The batoid fishes (skates, rays) form a monophyletic clade within the subclass Elasmobranchii and exhibit a broad range of morphologies and corresponding ecologies. We hypothesized that their visual field characteristics would reflect their diverse morphology and ecology. This was tested by quantifying the monocular, binocular and cyclopean horizontal and vertical visual fields of four batoid species (*Raja eglanteria*, *Urobatis jamaicensis*, *Dasyatis sabina* and *Rhinoptera bonasus*) that encompassed a range from a basal skate to a more derived ray. The horizontal and vertical visual fields differed significantly among species; however, all species possessed horizontal anterior and dorsal binocular overlaps. *Urobatis jamaicensis*, a small reef-associated stingray, demonstrated a 360° panoramic visual field in the horizontal plane, and *R. bonasus*, a schooling benthopelagic ray, a 360° panoramic view in the vertical plane. Large anterior binocular overlaps were measured in *D. sabina* (72°) and *R. bonasus* (46°) but came at the expense of large posterior blind areas. The anterior binocular overlaps in *R. eglanteria* (28°) and *U. jamaicensis* (34°) were smaller but were coupled with large monocular fields that provided expansive peripheral views. The most phylogenetically basal species, the clearnose skate (*Raja eglanteria*), had the most reduced visual field in contrast to the more derived ray species. To our knowledge, this study represents the first comparative assessment of visual fields in basal vertebrates.

Key words: vision, elasmobranch, skate, ray, binocular, convergence, *Dasyatis sabina*, *Raja eglanteria*, *Rhinoptera bonasus*, *Urobatis jamaicensis*.

### INTRODUCTION

Elasmobranch fishes (sharks, skates and rays) were once mischaracterized as possessing a poorly developed visual system. However, elasmobranchs exhibit a variety of advanced visual features including mobile pupils, multiple visual pigments (requisite for color vision), prominent visual streaks (enhance visual acuity) and a moveable lens that facilitates accommodation (Gruber, 1977; Hueter et al., 2004). These are characteristics of a much more complex system than previously reported (Hueter, 1991). Despite recent advances in our understanding of elasmobranch vision, numerous aspects remain unexplored, including such fundamental elements as the extent of the visual field.

An organism's visual field is the entire expanse of space visible at a given instant without moving the eyes. There are three measures of the visual field, which include the field of view of a single eye (monocular); the combined field of view of both eyes (cyclopean); and the overlap of the monocular fields (binocular). The point at which the monocular visual fields overlap is termed the binocular convergence point, and the distance from this point to the central point between the eyes (in the transverse plane) is called the convergence distance. A relatively short convergence distance provides depth perception beginning closer to the eyes, whereas with a longer convergence distance binocular vision is achieved further from the eyes.

The visual field is an integral component of the visual sensory system and is central to an organism's perception of its environment. Herbivorous animals that are heavily preyed upon often possess laterally positioned eyes with large monocular fields that facilitate motion detection of predators (Guillemain et al., 2002). By contrast, predators typically have frontally positioned

eyes with a large binocular overlap to facilitate accurate depth perception, which is vital for spatially tracking and acquiring prey (Blumstein et al., 2000).

Surprisingly, the importance of the visual field appears to have been overlooked as data on the extent of the monocular and binocular visual fields of vertebrates are limited to a small group including rabbits (Hughes, 1972), rats (Hughes, 1979), humans (Emsley, 1948), frogs and toads (Collett, 1977; Fite, 1973) and avians (Martin, 1999), with most visual field assessments limited to birds. Among aquatic organisms, the visual field has again been determined in relatively few species, including the harbor seal (Hanke et al., 2006), cuttlefish (Watanuki et al., 2000), parrotfish (Rice and Westneat, 2005), spiny dogfish (Harris, 1965) and lemon shark (Hueter and Gruber, 1982). Because visual fields have been examined in so few species and very few closely related species, the lack of cohesion and comparable methods have hindered the ability to formulate and test hypotheses regarding evolutionary adaptations of visual fields within phylogenetic and ecological contexts. Therefore, we chose to examine visual fields within a monophyletic clade of morphologically and ecologically diverse aquatic vertebrates, the batoid fishes.

Batoid fishes are dorsoventrally flattened elasmobranchs that constitute a monophyletic group nested within the shark clade (Douady et al., 2003). There are over 500 batoid species that exhibit tremendous diversity in head morphology, eye position, swimming behavior and ecology (Fig. 1). We hypothesized that visual field topography would correlate with all of these factors. To test this hypothesis we selected four representative species that differ in those characteristics and for which a well-determined phylogeny exists (Fig. 1).

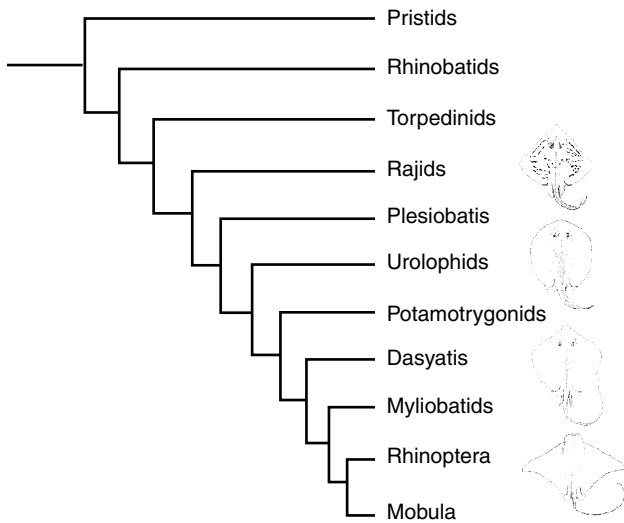


Fig. 1. Phylogeny of batoid fishes [based on Shirai (Shirai, 1996) and Sasko et al. (Sasko et al., 2006)] depicting the most basal skate (*Raja eglanteria*), intermediate rays (*Urobatis jamaicensis* and *Dasyatis sabina*) and most derived ray (*Rhinoptera bonasus*). Line drawings of batoids are modified from Bigelow and Schroeder (Bigelow and Schroeder, 1953).

#### ***Raja eglanteria***

The clearnose skate (*Raja eglanteria* Bosc 1802; Rajidae) is the most phylogenetically basal species in this study (Akbulut, 2006; McEachran and Dunn, 1998). The skate is a sub-tropical demersal, benthic forager found in the inshore areas of the western Atlantic and northeastern Gulf of Mexico (Smith, 1997; Stehmann and McEachran, 1978). It has low-profile dorsally positioned eyes set upon a dorso-ventrally compressed disk mottled with dark irregular markings (presumably for camouflage). Based upon the position of the eyes and the presence of cryptic markings, we predicted that *R. eglanteria* would have large lateral monocular fields for vigilance against predators, and its sedentary benthic lifestyle would not necessitate a large anterior binocular overlap.

#### ***Urobatis jamaicensis***

The yellow stingray (*Urobatis jamaicensis* Cuvier 1816; Urolophidae) is a small tropical, reef- and seagrass-associated ray that commonly buries itself under sand or lies sedentary in seagrass (Young, 1993). It is found along the western Atlantic from North Carolina to northern South America in a depth range of 1–25 m (Smith, 1997). Its body has yellow coloration with elaborate white spotting, most probably associated with camouflage. It is a benthic forager and has been documented to raise the anterior portion of its disk to attract refuge-seeking prey items (Robins and Ray, 1986). The dorsally positioned eyes are periscopic, enabling them to protrude above the substrate when the ray is buried. Based upon the eye position and presence of camouflage, we predicted that *U. jamaicensis* is heavily preyed upon and would be vigilant against predators. Therefore, it likely possesses large lateral monocular fields, including good overhead and binocular vision.

#### ***Dasyatis sabina***

The Atlantic stingray (*Dasyatis sabina* Leseur 1824; Dasyatidae) is a medium-sized subtropical ray with dorsally positioned eyes, a prominent triangular snout and a counter-shaded disk with the dorsal surface a deep brown and the ventral surface white. It inhabits coastal lagoons and seagrass habitats shallower than 25 m

(Snelson et al., 1988) from the Gulf of Mexico, and Chesapeake Bay through southern Florida, where it feeds upon benthic invertebrates (Michael, 1993; Cook, 1994). It is taxonomically intermediate within the assemblage and demonstrates an undulatory/oscillatory swimming pattern that allows for fast continuous locomotion (Rosenberger, 2001a). Because of its fast swimming and frontally canted eyes, we predicted that *D. sabina* would have a large binocular overlap and good overhead vision for predator detection.

#### ***Rhinoptera bonasus***

The cownose ray (*Rhinoptera bonasus* Mitchill 1815; Myliobatidae) is the most derived ray in the assemblage and possesses several attributes that distinguish it from the other species. It is a large tropical ray that inhabits the eastern and western Atlantic, Gulf of Mexico and northern South America in waters shallower than 22 m (Robins and Ray, 1986). It is the only species with laterally positioned eyes, the only one to exhibit schooling behavior, the only benthopelagic ray, and the only species to exhibit true oscillatory swimming. The head extends rostrally well beyond the margins of the pectoral fins, and the laterally placed eyes provide the potential for vision ventral to the body. Because of its propensity to form large schools in the water column, we predicted that *R. bonasus* would have binocular vision dorsally, anteriorly and ventrally.

The goal of this study was to quantify the horizontal and vertical visual fields of four batoid species. We asked three primary questions: (1) how do visual fields differ among species that possess different head morphology and eye position, (2) how do their visual fields correlate with their behavioral ecology and (3) are similarities in visual fields retained in morphologically similar, yet phylogenetically distant, species of skate and ray?

## **MATERIALS AND METHODS**

### **Experimental animals**

All experimental animals were collected in the near shore of FL, USA, except for *R. eglanteria*, which was obtained from a breeding population housed at Mote Marine Laboratory, Sarasota, FL, USA. Animals were maintained in flow-through aquaria and fed to satiation daily, until utilized for vision trials. Experimental animal protocols were approved and followed under Florida Atlantic University IACUC # A06-09 and Mote Marine Laboratory IACUC # 06-07-SK1. Data on sample size and morphometrics are provided in Table 1.

### **Experimental apparatus**

An electroretinogram (ERG) technique was utilized to determine the extent of the horizontal and vertical visual fields. The ERG uses a recording electrode placed within the vitreal component of the eye to detect a change in electrical potential when light impinges upon the photoreceptive layer of the retina. The experimental light source was a white light-emitting diode (LED) (5 mm diameter/1100 millicandella) that delivered a beam of light through an acrylic cylinder, which was beveled to terminate in a 1-mm-wide slit. The acrylic cylinder light guide was painted black so light could emanate only from the slit. The light guide was mounted within a mobile track that was fitted upon a protractor, which permitted the light guide to be freely rotated around the eye in exact degree increments. The protractor light guide apparatus was positioned with a micromanipulator over the dorsal surface of the batoid with the center of the protractor carefully aligned at the lateral margin of the cornea. This permitted the light guide to be

Table 1. Morphometric summary data for all batoid species

Family Species	Rajidae <i>Raja eglanteria</i>	Urolophidae <i>Urobatis jamaicensis</i>	Dasyatidae <i>Dasyatis sabina</i>	Rhinopterae <i>Rhinoptera bonasus</i>
N	6	6	7	6
Disc width (cm)	22.9±0.8	17.7±0.4	24.6±0.6	40.0±1.9
Habitat	Demersal	Reef/seagrass	Demersal	Benthopelagic
Eye position	Dorsal	Dorsal	Dorsal	Lateral
Inter-ocular distance (cm)	2.8±0.6	3.0±0.1	5.2±0.2	7.0±0.4
Horizontal plane				
Monocular (°)	186.0±2.6	198.0±2.0	199.0±3.1	184.0±2.6
Binocular (°)	28.0±2.4	34.0±3.2	72.0±6.7	46.0±4.7
Cyclopean (°)	344.0±3.9	360.0±0.3	327±6.1	321±2.3
Standardized				
Anterior convergence distance (cm)	10.6±0.8	8.6±0.8	3.7±0.5	6.3±0.7
Anterior blind area (cm <sup>2</sup> )	13.2±1.0	10.8±1.0	4.7±0.7	7.9±0.9
Anterior eye rotation (°)	8.1±1.2	8.1±0.6	18.3±0.9	7.5±1.4
Posterior eye rotation (°)	12.0±0.6	15.0±1.0	12.1±1.4	5.8±1.1
Vertical plane				
Monocular (°)	104.0±0.7	132.0±1.1	115.0±1.4	196.0±2.6
Binocular (°)	8.0±1.5	38.0±2.6	20.0±2.7	12.0±2.5
Cyclopean (°)	200.0±0.5	224.0±2.5	211.0±0.7	360.0±0.0
Standardized				
Dorsal convergence distance (cm)	43.9±9.0	7.4±0.5	15.7±2.6	35.7±11.3
Dorsal blind area (cm <sup>2</sup> )	54.9±11.3	9.2±0.6	19.6±3.2	44.6±14.1

Values represent mean ± s.e.m.

rotated around the eye in the horizontal plane and to deliver a vertical slit of light that illuminated the cornea from the dorsal to the ventral margins. To determine the vertical visual field, the protractor device was repositioned orthogonally to allow the light guide to rotate around the eye in the vertical plane. We did not determine the visual field in the sagittal plane because the dorsal positioning and dorsal exposure of the eye resulted in all positive responses in that plane (pilot data not shown).

The ERG was recorded with 100 µm tip glass electrodes filled with 2 mol l<sup>-1</sup> NaCl in 5% agar. A recording electrode was placed within the vitreal component of the eye, and a reference electrode upon the skin of the batoid. The electrodes were differentially amplified to detect the electrical potential of the photoreceptors when light impinged upon the retina. The output from the electrodes was amplified (100–1000×) and filtered (low-pass 1 kHz, high-pass 0.1 Hz) with a differential amplifier (DP-304; Warner Instruments, Hamden, CT, USA). The data were acquired and digitized with Power Lab<sup>®</sup> 16/30 model ML 880 (AD Instruments, Colorado Springs, CO, USA) and recorded at 1 kHz using Chart<sup>™</sup> Software (AD Instruments).

#### Experimental protocol

To assess the visual field, animals were anesthetized with tricaine methanesulphonate (MS-222) (1:15 000 w/v). After respiration ceased (2–4 min), animals were quickly transferred to an acrylic experimental tank (89×43×21 cm) and secured with Velcro<sup>®</sup> straps to a submerged plastic stage. The animal was immediately fitted with an oral ventilation tube that delivered a recirculating maintenance dose (1:20 000 w/v) of MS-222 throughout the experiment. The spiracles were plugged with small form-fitting pieces of sponge to ensure that water flowed over the gills. Micromanipulators were then fixed over the tank to hold the two electrodes and the protractor/light guide apparatus. Light leakage into the room was eliminated and a light-tight box was created to cover the computer and experimenter recording the ERG data. The animals were

allowed to adapt to the darkened experimental room for 30 min to ensure maximal pupillary dilation and therefore greatest retinal exposure (Cohen and Gruber, 1977).

After full dark adaptation, the trial began with a computer-controlled 2-s flash of the LED directed at the pupil. A clear ERG response was obtained immediately upon activation of the LED (Fig. 2). After a 3-min delay (to allow the eye to recover), the light guide was repositioned in 10° increments and the procedure repeated. A low-power hand-held red LED torch was used by the experimenter to illuminate the protractor and reposition the light guide. The visual field was determined by directing the light around the eye and establishing whether or not there was an ERG waveform response. As the limit of the field was approached, the testing was reduced from 10 to 1° increments. The last angle to produce an ERG response was defined as the limit of the visual field. All measures were taken on anesthetized animals whose eyes were in a static relaxed state. At the conclusion of each experiment, animals were ventilated with fresh seawater and all animals revived and recovered fully.

#### Analysis

The horizontal and vertical visual field limits were defined by four demarcations: anterior horizontal (AH), posterior horizontal (PH), dorsal vertical (DV) and ventral vertical (VV). In the horizontal plane, 0° was set anterior to the eye, 90° directly lateral to the eye, and 180° posterior to the eye. In the vertical plane, 0° was dorsal to the eye, 90° directly lateral to the eye, and 180° ventral to the eye (Fig. 3). Because the pectoral fins of *R. eglanteria*, *D. sabina* and *U. jamaicensis* occlude a continuous ventral visual field, the ventral visual limit was determined, in addition to the ERG, by digitally photographing each individual head-on and using the software Image J (Rasband, 1997) to calculate the angle from the midline of the eye to the disc wingtip.

The convergence distance and blind area were calculated for each individual based upon the inter-ocular distance and visual field demarcations. To facilitate comparison of visual field parameters,

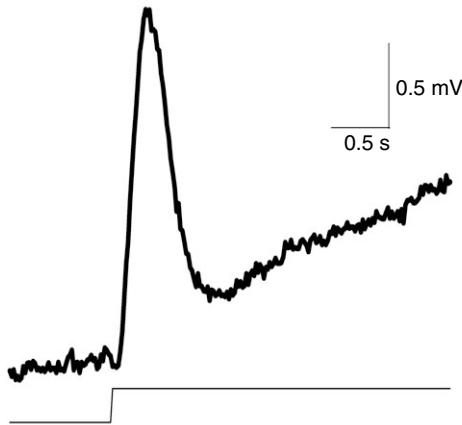


Fig. 2. The electroretinogram waveform response of *Raja eglanteria* to light stimulus. The presence of a positive waveform to the flash was the criterion used to determine the functional visual fields of the batoid fishes. Step bar indicates onset and duration of light flash.

we also calculated convergence distance and blind area for each individual by utilizing a standardized inter-ocular distance (5 cm, the mean of all species combined), thereby eliminating animal size as a confounding factor.

To determine the extent of eye rotation, we used surgical forceps to fully retract the medial and lateral rectus muscles for a minimum of six freshly dead individuals of each species. Eyes were photographed dorsally in the natural, converged and diverged positions, and the angle of rotation determined using Image J software (Rasband, 1997).

To determine differences in the visual fields among the four batoid species, the monocular and binocular visual fields, convergence distance, blind area, visual field demarcations (AH, PH, DV, VV) and eyeball rotations of all individuals were compared using one-way ANOVA (Systat Software, Inc., San Jose, CA, USA) with pairwise multiple comparisons by Tukey *post-hoc* tests. The cyclopean visual field data were non-normal and analyzed with a Kruskal-Wallis ANOVA on ranks with multiple comparisons using Dunn's method.

## RESULTS

The ERG technique permitted the direct measurement of the functional visual field in the horizontal and vertical planes. The visual field demarcations in both planes differed significantly among the four batoid species (Fig. 3) (horizontal: anterior ANOVA,  $F=17.0$ ,  $P<0.001$ ; posterior ANOVA,  $F=19.4$ ,  $P<0.001$ ) (vertical: dorsal ANOVA,  $F=28.2$ ,  $P<0.001$ ; ventral ANOVA,  $F=1599.7$ ,  $P<0.001$ ). Pairwise comparisons are illustrated in Fig. 3. Based upon the visual field demarcations, the monocular, binocular and cyclopean visual fields were calculated for all species in the study (Table 1). The visual fields in both the horizontal and vertical planes differed significantly among the four species (Fig. 4) (horizontal ANOVA,  $F=8.9$ ,  $P<0.001$ ; vertical ANOVA,  $F=620.5$ ,  $P<0.001$ ). Pairwise comparisons are outlined in Table 2.

The visual field demarcations and inter-ocular distance (cm) for each individual were utilized to construct the convergence distance (cm) and blind area ( $\text{cm}^2$ ). Both convergence distance and blind area were calculated using a standardized inter-ocular distance to eliminate the effects of body size (Table 1). The standardized convergence distance and blind area differed significantly among the four batoid species in both the horizontal and vertical planes

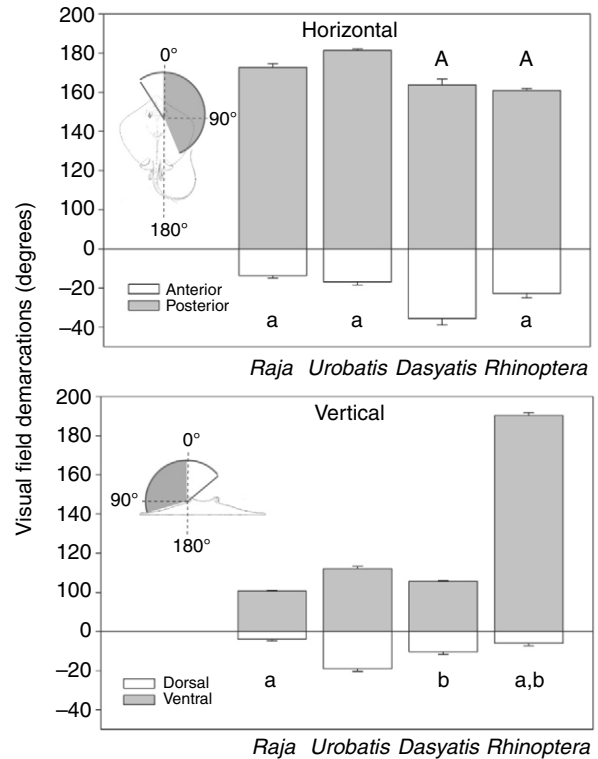


Fig. 3. The mean value ( $\pm$  s.e.m.) of each visual field demarcation as measured on both the horizontal and vertical planes. Bars that share the same upper or lower case letter do not differ significantly.

(Fig. 4) (standardized convergence distance: horizontal ANOVA,  $F=16.0$ ,  $P<0.001$ ; vertical ANOVA,  $F=14.0$ ,  $P<0.001$ ) (blind area: horizontal ANOVA,  $F=16.0$ ,  $P<0.001$ ; vertical ANOVA,  $F=14.0$ ,  $P<0.001$ ). Pairwise comparisons are provided in Table 2.

The visual field topography changes with eyeball rotation; therefore, we measured the maximum anterior and posterior eyeball rotation in the horizontal plane (Table 1). The degree of eyeball rotation differed significantly among species in both anterior (ANOVA,  $F=22.1$ ,  $P<0.001$ ) and posterior directions (ANOVA,  $F=11.5$ ,  $P<0.001$ ). Pairwise comparisons are provided in Table 2. Given the data on eyeball rotation, we constructed the dynamic visual fields with the eyes converged (positioned anterior) and with the eyes diverged (positioned posterior) (Fig. 5).

## DISCUSSION

In an effort to bring broader relevance to our findings, we contrasted batoid visual fields to the visual field types described for birds. In birds, Type I visual fields are found in species with a binocular overlap of 20–30° that commonly lunge and peck and rely on vision for information on locomotion and feeding. Type II visual fields are characterized by a binocular overlap of less than 10° and are commonly found in tactile feeders that rely less on vision for detection and procurement of food and more for vigilance against predators and detecting conspecifics. Type III visual fields consist of broad binocular overlaps ( $\approx 50^\circ$ ) that are coupled with large posterior blind areas and are seen in fast-moving predators that may simultaneously utilize other sensory modalities (Martin and Katzir, 1999) just prior to prey capture. Although anatomical features, such as the structure of the retina, differ between birds and elasmobranchs, both groups face the common challenges of predator vigilance and optimizing frontal



vision for locomotion, feeding and mate detection. Therefore, it would not be surprising to find the convergence of visual field types in terrestrial and aquatic organisms. The visual field

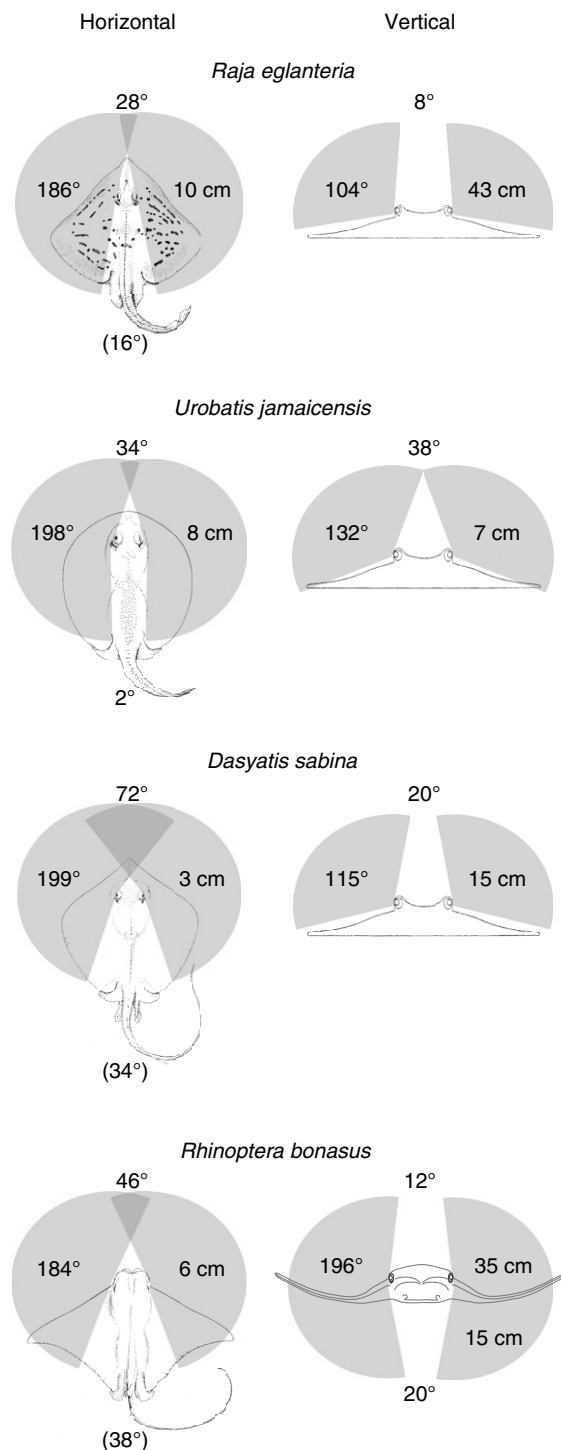


Fig. 4. The static functional horizontal and vertical visual fields of four batoid species. Values within the shaded area represent monocular visual fields (left side) and the standardized convergence distance (right side). Values shown outside of the shaded areas represent binocular overlaps, and values in parentheses indicate blind areas. *Urobatis jamaicensis* possesses a 360° horizontal visual field, and *Rhinoptera bonasus* possesses a 360° vertical visual field. Line drawings of batoids are modified from previous publications (Bigelow and Schroeder, 1953; Nicol, 1978).

characteristics of both *U. jamaicensis* and *R. eglanteria* were similar to the Type I and II visual fields in birds, whereas *D. sabina* and *R. bonasus* were more similar to Type III visual fields. Both *U. jamaicensis* and *R. eglanteria* possess distinct body markings and elaborate pupillary structures (both presumably for camouflage), which suggests that predator vigilance is paramount, a behavioral characteristic found in birds with Type II visual fields. Additionally, *D. sabina* and *R. bonasus* move faster than the other species and may utilize other sensory modalities to search for prey, which is a shared behavioral characteristic of birds that possess Type III visual fields.

### Morphology

All four batoid species possessed horizontal anterior binocular overlaps that confer frontal vision. The overlaps were largest in *R. bonasus* and *D. sabina* and were comparable to those of species with nearly frontal-facing eyes such as the frog *Rana pipiens* (90°) (Grobstein et al., 1980). However, the large binocular overlaps apparently came at the expense of reduced posterior visual fields, as *D. sabina* and *R. bonasus* had the largest posterior blind areas. The horizontal anterior binocular overlaps in *U. jamaicensis* and *R. eglanteria* were smaller than the other species but large enough to allow visually guided locomotion and feeding. *Urobatis jamaicensis* was the only species to have a full 360° panoramic view on the horizontal plane. A dorsal binocular overlap was measured in all species, and *U. jamaicensis* had the largest overlap (38°). *Rhinoptera bonasus* had the greatest morphological departure from all species in the study, and its laterally positioned eyes, set anterior to the pectoral wings, allow for a full 360° vertical cyclopean field around the head.

*Dasyatis sabina* is the only batoid for which there are some existing visual field data in the literature (Nicol, 1978). The visual fields in Nicol's study were determined by utilizing photographs of the eyes. Despite differences in methodology, the monocular visual field of *D. sabina* obtained in the present study (199°) is very similar to that reported by Nicol (190°). Sivak described a ramp retina in *D. sabina* (Sivak, 1975), which permits simultaneous focus of images at various distances, and Logiudice and Laird reported the presence of rods, cones and a horizontal visual streak (Logiudice and Laird, 1994). The horizontal visual streak would likely enhance the visual acuity within the horizontal monocular visual field of *D. sabina*, which was the largest measured in this study.

The extent of exposure of the globe of the eye and the position of the eye within the socket partially determine the expansiveness of the visual field. The eye of *U. jamaicensis* protrudes from the eye cup more than other species, and the posterior and dorsal skin is positioned further from the globe of the eye. This direct exposure may contribute to *U. jamaicensis* possessing the widest measured vertical binocular overlap. The eye of *D. sabina* is canted slightly forward and skin surrounding the anterior portion of the eye is retracted, resulting in the largest measured anterior binocular overlap.

Eyeball rotation changes visual field topography, and all four species demonstrated anterior binocular convergence with the eyes in the relaxed and converged states. However, even in the diverged state, *D. sabina* and *R. bonasus* still retained anterior binocular convergence but they did not achieve posterior binocular convergence. By contrast, the 16° posterior blind area in *R. eglanteria* is abolished and replaced by an 8° binocular overlap when the eyes are moved from a relaxed to a diverged state (Fig. 5). Even in the diverged state, *R. eglanteria* retains anterior binocular overlap, providing it with full 360° vision.

Table 2. Statistical significance of pairwise comparisons (*P*-values) of the visual field parameters for all batoid species

		Horizontal			Vertical		
		Monocular			Monocular		
	<i>Raja</i>	<i>Urobatis</i>	<i>Dasyatis</i>	<i>Raja</i>	<i>Urobatis</i>	<i>Dasyatis</i>	
<i>Urobatis</i>	0.029	–	–	<0.001	–	–	
<i>Dasyatis</i>	0.012	NS	–	<0.001	<0.001	–	
<i>Rhinoptera</i>	NS	0.006	0.002	<0.001	<0.001	<0.001	
		Binocular			Binocular		
	<i>Raja</i>	<i>Urobatis</i>	<i>Dasyatis</i>	<i>Raja</i>	<i>Urobatis</i>	<i>Dasyatis</i>	
<i>Urobatis</i>	NS	–	–	<0.001	–	–	
<i>Dasyatis</i>	<0.001	<0.001	–	0.007	<0.001	–	
<i>Rhinoptera</i>	NS	NS	0.005	NS	<0.001	NS	
		Cyclopean			Cyclopean		
	<i>Raja</i>	<i>Urobatis</i>	<i>Dasyatis</i>	<i>Raja</i>	<i>Urobatis</i>	<i>Dasyatis</i>	
<i>Urobatis</i>	NS	–	–	<0.05	–	–	
<i>Dasyatis</i>	NS	<0.05	–	NS	NS	–	
<i>Rhinoptera</i>	NS	<0.05	NS	<0.05	NS	<0.05	
		Convergence distance			Convergence distance		
	<i>Raja</i>	<i>Urobatis</i>	<i>Dasyatis</i>	<i>Raja</i>	<i>Urobatis</i>	<i>Dasyatis</i>	
<i>Urobatis</i>	NS	–	–	<0.001	–	–	
<i>Dasyatis</i>	NS	NS	–	NS	0.001	–	
<i>Rhinoptera</i>	NS	0.021	0.002	NS	<0.001	0.017	
		Blind area			Blind area		
	<i>Raja</i>	<i>Urobatis</i>	<i>Dasyatis</i>	<i>Raja</i>	<i>Urobatis</i>	<i>Dasyatis</i>	
<i>Urobatis</i>	NS	–	–	<0.001	–	–	
<i>Dasyatis</i>	NS	NS	–	NS	<0.001	–	
<i>Rhinoptera</i>	<0.001	<0.001	<0.001	0.001	<0.001	0.004	
		Anterior eye rotation			Posterior eye rotation		
	<i>Raja</i>	<i>Urobatis</i>	<i>Dasyatis</i>	<i>Raja</i>	<i>Urobatis</i>	<i>Dasyatis</i>	
<i>Urobatis</i>	NS	–	–	NS	–	–	
<i>Dasyatis</i>	<0.001	<0.001	–	NS	NS	–	
<i>Rhinoptera</i>	NS	NS	<0.001	0.005	<0.001	0.004	

NS = not significant.

### Locomotion

The convergence distance and blind areas are measures of special interest within the context of locomotion. In fast-moving species, the possession of short convergence distances and small blind areas would confer an advantage in optimizing visual information. The four batoids demonstrate three distinct locomotory patterns (Rosenberger, 2001a). Both *R. eglanteria* and *U. jamaicensis* utilize an undulatory (more than one wave present on the fin at a time) swimming pattern that is associated with a more sedentary lifestyle. The skate had the longest horizontal anterior convergence distance (10 cm), followed by *U. jamaicensis* (8 cm). For both of these sedentary species, binocular vision starting near the head may not be as important as for faster swimming species. *Dasyatis sabina*, which has a large anterior binocular overlap and the shortest horizontal anterior convergence distance (3 cm), demonstrates an intermediate swimming pattern that is a blend of undulation and oscillation (between half a wave and one wave present on the fin) (Rosenberger, 2001a). The most derived ray in the assemblage, *R. bonasus*, is the only one to exhibit true oscillatory swimming (fin moves up and down with less than half a wave present on the fin)

and has a large anterior binocular overlap similar to that found in *D. sabina*. This binocular overlap is important, as they tend to form large schools in the water column (Blaylock, 1989).

### Ecology

The habitat associations of the batoids are different and correlate to aspects of their visual fields. *Raja eglanteria* is demersal, inhabiting mudflats, estuaries and rubble bottoms, which allows the skate to bury and protrude the eyes from the bottom (Bigelow and Schroeder, 1953). *Urobatis jamaicensis* often buries in the substrate (Michael, 1993), giving its periscopic eyes a panoramic 360° view of the complex reef environment. The large anterior binocular overlap found in *D. sabina* is beneficial as it negotiates turbid shallow coastal lagoons with sea grass and sandy bottoms (Snelson et al., 1988). *Rhinoptera bonasus* is the only benthic-pelagic ray with ventral binocular vision, which permits viewing of the oyster beds and estuarine sea grass common to its habitat (Blaylock, 1989). Additionally, *R. bonasus* is known to school in large numbers (Clarke, 1963), and the 360° vertical field would allow for viewing of conspecifics while swimming.

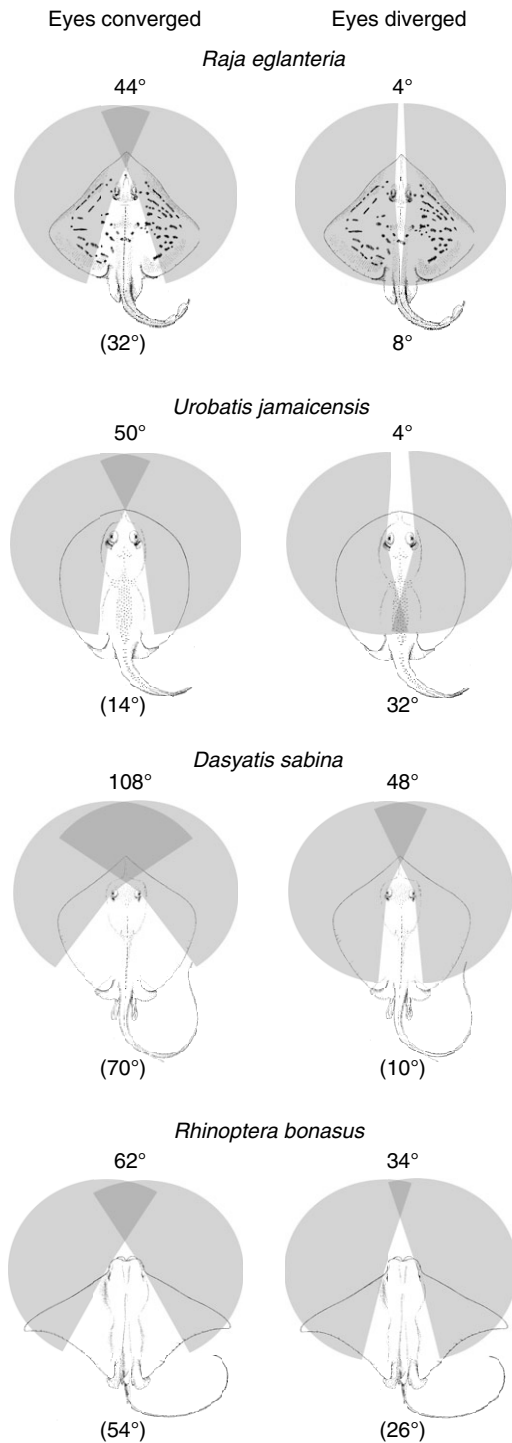


Fig. 5. Visual fields and eye movements. The dynamic horizontal visual fields of four batoid species when the eyes are fully converged and fully diverged. The values at the anterior and posterior margins of the disk indicate the degrees of binocular overlap, or blind area if in parentheses.

All three demersal species bury themselves in the substratum, presumably to avoid detection by predators. Both *R. eglanteria* and *U. jamaicensis* possess camouflage coloration and an elaborate pupillary operculum (Fig. 6). The pupillary operculum has been suggested to enhance camouflage of the eyes in these substrate-



Fig. 6. The elaborate pupillary operculum structures that allow for the control of light entering the eyes of *R. eglanteria* (right) and *U. jamaicensis* (left).

dwelling species (Douglas et al., 2002) in addition to controlling the amount of light that enters the eye and maintaining a shallow depth of field (Murphy and Howland, 1991; Sivak and Luer, 1991). We predicted that the demersal species should therefore possess good overhead vision to enable them to remain vigilant while buried. We found that *U. jamaicensis* and *D. sabina* both possessed a greater (larger) dorsal visual field than the clearnose skate. This may be a reflection of the skate's basal phylogenetic position or the evolution of more periscopically positioned eyes in the more recently derived rays.

Because the three demersal species feed primarily upon benthic infauna, vision does not likely play an important role in prey detection. Indeed, with their dorsally positioned eyes and ventrally positioned mouth, these species can never see what they eat and rely instead upon exquisitely sensitive touch receptors (Maruska and Tricas, 1998) and electroreceptors (Sisneros and Tricas, 2002; Blonder and Alevizon, 1988) to localize their prey. Unlike the benthically associated species, *R. bonasus* often swims in the water column (Blaylock, 1989), where its lateral line and electrosensory systems, which both operate at close range, would be unable to provide it with spatial information about the location of its benthic prey. The diet of *R. bonasus* is composed primarily of benthic mollusks with a small percentage of teleosts (Smith and Merriner, 1985). Therefore, the expanded ventral visual field may enable *R. bonasus* to visually locate the oyster and clam beds upon which it feeds.

*Raja eglanteria* was discovered to have the most reduced visual field in comparison with the more derived rays. However, the clearnose skate does possess one specialization that the rays do not: the translucent panes of rostral tissue from which they derive their common name. To our knowledge, the functional significance of the translucent rostral tissue has never been addressed in the literature. The fact that the horizontal visual field overlaps the rostral panes led us to hypothesize that *R. eglanteria* may have the ability to see through its own translucent tissue. To this end, we directed a beam of light from beneath the translucent pane and impinged the light onto the retina and recorded a positive ERG response. This response simply demonstrates that light can be detected through the rostral tissue; whether this corresponds to a visual or behavioral function remains to be tested. However, it is

interesting to note that the mouth of *R. eglanteria* is located ventrally and immediately posterior to the rostral panes. These windows may allow for last-second visual tracking and acquisition of prey. Although clear image formation through the panes is unlikely, they may at least permit the detection of motion. Rostral translucency is not limited to this species and is found within several skate species and has independently evolved in the guitarfish (Rhinobatidae). A future goal is to investigate a possible visual function of these panes.

Whereas vision may not play as important a role as electroreception in locating benthic or cryptic prey, it may be most important in vigilance against predators and in detecting potential mates. Both *R. eglanteria* and *U. jamaicensis* were determined to have large monocular fields and an approximately 20–30° binocular overlap. This has been described as the optimal functional width in birds, as it allows sufficient optic flow field information to ensure accurate locomotion and prey capture while still maximizing the peripheral view (Martin, 2007). The horizontal anterior binocular overlap in *D. sabina* and *R. bonasus* are large ( $\approx 50^\circ$ ) and are coincident with large blind areas behind the head. This Type III visual field is characteristic of predators with large eyes that show a reduction in vigilance behavior. This is supported by the fact that neither of these species possesses the elaborate body camouflage or pupillary operculum structures that are present in *R. eglanteria* and *U. jamaicensis*.

### Evolution

The finding that the most limited visual field was present in the most basal species in our assemblage, *R. eglanteria*, has relevance in an evolutionary context. All of the rays in this study had larger visual fields on the horizontal plane and, in the case of *R. bonasus*, in the vertical plane. This discovery suggests that skates may have had a smaller visual field that expanded during the radiation of the rays, which in turn shifted the visual field to suit each species' particular ecological niche. However, since the visual field of only one skate was determined in this study, more assessments are needed to resolve the question.

To determine whether a species' visual field shifts as a result of its ecological niche, it would be interesting to determine visual fields of other species that are further morphological departures from the species examined in the present study. For example, the manta (*Manta birostris*), a huge derived pelagic ray, has truly unique head morphology with large cephalic lobes that aid in feeding. The manta has laterally positioned eyes, yet they are canted slightly forward, which most likely results in a binocular overlap that would be beneficial to the ray as it continually swims and feeds on plankton. However, unfurling the cephalic lobes during feeding may partially occlude the frontal visual field. To compensate for this visual field reduction, the manta may rotate the eyes anteriorly, as independent eye movement has been observed in this species in the wild (Coles, 1916).

A visual field assessment of guitarfish would be relevant, as the Atlantic guitarfish (*Rhinobatos lentiginosus*) and the shovelnose guitarfish (*Rhinobatos productus*) both possess rostral translucency similar to that observed in *R. eglanteria*. If there is a visual function associated with the presence of rostral translucency, a visual field overlap of the rostral tissue would be predicted, as was demonstrated in *R. eglanteria*.

It is possible that the benthic batoids have a capacity for greater ventral visual fields and that the constraint is merely due to occlusion by the pectoral fins and not a limitation of the visual apparatus. This could be verified by examining a morphologically

similar species that is not constrained to a benthic environment and demonstrates a more oscillatory swimming pattern. The pelagic stingray, *Pteroplatytrygon violacea*, has a nearly worldwide distribution and is commonly found in the top 100 m over deep waters (Mollet, 2002). It is closely related to *D. sabina* and has similar body morphology and eye position. However, *P. violacea* is pelagic and its pectoral fins are wider and more flexible than those of *D. sabina* (Rosenberger, 2001a). The greater ventral excursion of the pectoral fins while swimming will likely result in an expanded ventral visual field.

The goals of the present study were to test whether visual fields varied among batoid species, if the extent of the visual fields correlated with their behavioral ecology, and if visual fields demonstrated greater similarity among closely related species compared with phylogenetically distant ones. The four batoid species in this study differ in head morphology, eye position (Compagno, 1977), pectoral fin locomotion (Rosenberger, 2001b), feeding dynamics (Dean et al., 2005; Smith and Merriner, 1985) and habitat associations (Snelson et al., 1988). Whereas our data suggest interesting correlations between visual fields and ecology, data from other species, especially those that possess morphological distinctions, are needed to definitively correlate the visual fields of elasmobranch fishes with aspects of their ecology.

Thanks to M. Kobza, L. Macesic, T. Meredith, A. Cornett, K. Smith, C. Bedore and J. Miedema for assistance during experimentation. Thanks to M. Royer and the Vertes lab at Florida Atlantic University for technical support. Thanks to Mote Marine Laboratory's staff: Dr C. Luer for the generous donation of the clearnose skates, and to J. Morris for collecting and housing the cownose rays used in this study and to Gumbo Limbo Research Station staff for housing all other species. We gratefully acknowledge Dusky Marine for our vessel and motor that were used in animal collection. D.M.McC. gratefully acknowledges financial support from PADI Project A.W.A.R.E., Florida Atlantic University's Graduate Fellowship for Academic Excellence and Newell Doctoral Fellowship, as well as the Boca Raton Junior Women's Club Scholarship.

### REFERENCES

- Akbulut, M. D. (2006). Specification of phylogenetic interrelations between skate-rays and sharks. *J. Evol. Biochem. Physiol.* **42**, 128-133.
- Bigelow, H. B. and Schroeder, W. C. (1953). Fishes of the Gulf of Maine. *Fish. Bull. Fish Wildl. Serv.* **53**.
- Blaylock, R. A. (1989). A massive school of cownose ray, *Rhinoptera bonasus* (Rhinopteriidae), in lower Chesapeake Bay, Virginia. *Copeia* **3**, 744-748.
- Blonder, B. I. and Alevizon, W. S. (1988). Prey discrimination and electroreception in the stingray *Dasyatis sabina*. *Copeia* **1**, 33-36.
- Blumstein, D. T., Daniel, J. T., Griffin, A. S. and Evans, C. S. (2000). Insular tamar wallabies (*Macropus eugenii*) respond to visual but not acoustic cues from predators. *Behav. Biol.* **11**, 528-535.
- Clark, E. (1963). Massive aggregations of large rays and sharks in and near Sarasota, Florida. *Zoologica* **48**, 61-64.
- Cohen, J. L. and Gruber, S. H. (1977). Spectral sensitivity and purkinje shift in the retina of the lemon shark, *Negaprion brevirostris* (Poey). *Vis. Res.* **17**, 787-792.
- Coles, R. J. (1916). Natural history notes on the devil-fish, *Manta birostris* (Walbaum) and *Mobula olfersi* (Müller). *Bull. Am. Mus. Nat. Hist.* **35**, 649-657.
- Collett, T. (1977). Stereopsis in toads. *Nature* **267**, 349-351.
- Compagno, L. V. (1977). Phyletic relationships of living sharks and rays. *Am. Zool.* **17**, 303-322.
- Cook, D. A. (1994). Temporal patterns of food habits of the Atlantic stingray, *Dasyatis sabina* (LeSeur 1884), from the banana river lagoon, Florida. MS thesis, Florida Institute of Technology, USA.
- Dean, M. N., Wilga, C. D. and Summers, A. P. (2005). Eating without hands or tongue: specialization, elaboration, and the evolution of prey processing mechanisms in cartilaginous fish. *Biol. Lett.* **1**, 357-361.
- Douady, C. J., Dosay, M., Shivji, M. S. and Stanhope, M. J. (2003). Molecular phylogenetic evidence refuting the hypothesis of Batoidea (rays and skates) as derived sharks. *Mol. Phylogenet. Evol.* **26**, 215-221.
- Douglas, R. H., Collin, S. P. and Corrigan, J. (2002). The eyes of suckermouth armoured catfish (Loricariidae, subfamily Hypostomus): pupil response, lenticular longitudinal spherical aberration and retinal topography. *J. Exp. Biol.* **205**, 3425-3433.
- Emsley, H. H. (1948). *Visual Optics* (4th edn). London: Hatton.
- Fite, K. V. (1973). The visual fields of the frog and toad: a comparative study. *Behav. Biol.* **9**, 707-718.
- Grobstein, P., Comer, C. and Kostyk, S. (1980). The potential binocular field and its tectal representation in *Rana pipiens*. *J. Comp. Neurol.* **190**, 175-185.
- Gruber, S. H. (1977). The visual system of sharks: adaptations and capability. *Am. Zool.* **17**, 453-469.



- Guillemain, M., Martin, G. R. and Fritz, H.** (2002). Feeding methods, visual fields and vigilance in dabbling ducks (Anatidae). *Funct. Ecol.* **16**, 522-529.
- Hanke, W., Römer, R. and Denhardt, G.** (2006). Visual fields and eye movements in a harbor seal (*Phoca vitulina*). *Vis. Res.* **46**, 2804-2814.
- Harris, J. A.** (1965). Eye movements of the dogfish *Squalus Acanthis* L. *J. Exp. Biol.* **43**, 107-130.
- Hueter, R. E.** (1991). Introduction: vision in elasmobranchs. *J. Exp. Zool.* **256**, Suppl. 5, 1-2.
- Hueter, R. E. and Gruber, S. H.** (1982). Recent advances in studies of the visual system of the juvenile lemon shark (*Negaprion brevirostris*). *Fla. Sci.* **45**, 11-25.
- Hueter, R. E., Mann, D. A., Maruska, K. P., Sisneros, J. A. and Demski, L. S.** (2004). Sensory biology of elasmobranchs. In *Biology of Sharks and their Relatives* (ed. J. C. Carrier, J. A. Musick and M. R. Heithaus), pp. 326-368. New York: CRC Press.
- Hughes, A.** (1972). A schematic eye for the rabbit. *Vis. Res.* **12**, 123-128.
- Hughes, A.** (1979). A schematic eye for the rat. *Vis. Res.* **19**, 569-588.
- Logiudice, F. T. and Laird, R. J.** (1994). Morphology and density distribution of cone photoreceptors in the retina of the Atlantic stingray, *Dasyatis sabina*. *J. Morphol.* **221**, 277-289.
- Martin, G. R.** (1999). Optical structure and visual fields in birds: their relationship with foraging behaviour and ecology. In *Adaptive Mechanisms in the Ecology of Vision* (ed. S. N. Archer, M. B. A. Djamgoz, E. Loew, J. C. Partridge and S. Vallerga), pp. 485-508. Dordrecht: Kluwer.
- Martin, G. R.** (2007). Visual fields and their functions in birds. *J. Ornithol.* **148**, Suppl. 2, 547-562.
- Martin, G. R. and Katzir, G.** (1999). Visual field in short-toed eagles *Circaetus gallicus* and the function of binocularity in birds. *Brain Behav. Evol.* **53**, 55-66.
- Maruska, K. P. and Tricas, T. C.** (1998). Morphology of the mechanosensory lateral line system in the Atlantic stingray, *Dasyatis sabina*: the mechanotactile hypothesis. *J. Morphol.* **238**, 1-22.
- McEachran, J. D. and Dunn, K. A.** (1998). Phylogenetic analysis of skates, a morphologically conservative clade of elasmobranchs (Chondrichthyes: Rajidae). *Copeia* **2**, 271-290.
- Michael, S. W.** (1993). *Reef Sharks and Rays of the World*. Monterey, CA: Sea Challengers.
- Mollet, H. F.** (2002). Distribution of the pelagic stingray, *Dasyatis violacea* (Bonaparte, 1832), off California, Central America, and worldwide. *Mar. Freshw. Res.* **53**, 525-530.
- Murphy, C. J. and Howland, H. C.** (1991). The functional significance of crescent-shaped pupils and multiple pupillary apertures. *J. Exp. Zool.* **256**, Suppl. 5, 22-28.
- Nicol, J. C.** (1978). Studies on the eye of the stingaree *Dasyatis sabina*, with notes on other selachians. I. Eye dimensions, cornea, pupil and lens. *Contrib. Mar. Sci.* **21**, 89-102.
- Rasband, W. S.** (1997). *ImageJ*. Bethesda, MD: US National Institutes of Health.
- Rice, A. N. and Westneat, M. W.** (2005). Coordination of feeding, locomotor and visual systems in parrotfishes (Teleostei: Labridae). *J. Exp. Biol.* **208**, 3503-3518.
- Robins, C. R. and Ray, G. C.** (1986). *A Field Guide to Atlantic Coast Fishes of North America*. Boston: Houghton Mifflin Company.
- Rosenberger, L. J.** (2001a). Pectoral fin locomotion in batoid fishes: undulation versus oscillation. *J. Exp. Biol.* **204**, 379-394.
- Rosenberger, L. J.** (2001b). Phylogenetic relationships within the Stingray genus *Dasyatis* (Chondrichthyes: Dasyatidae). *Copeia* **3**, 615-627.
- Sasko, D. E., Dean, M. N., Motta, P. J. and Hueter, R. E.** (2006). Prey capture behavior and kinematics of the Atlantic cownose ray, *Rhinoptera bonasus*. *Zoology* **109**, 171-181.
- Shirai, S.** (1996). Phylogenetic interrelationships of Neoselachians (Chondrichthyes: Euselachii). In *Interrelationships of Fishes* (ed. M. L. J. Stiassny, L. R. Parenti and G. D. Johnson), pp. 9-34. San Diego: Academic Press.
- Sisneros, J. A. and Tricas, T. C.** (2002). Ontogenetic changes in the response properties of the peripheral electrosensory system in the Atlantic stingray (*Dasyatis sabina*). *Brain Behav. Evol.* **59**, 130-140.
- Sivak, J. G.** (1975). The accommodative significance of the "ramp" retina of the eye of the stingray. *Vis. Res.* **16**, 945-950.
- Sivak, J. G. and Luer, C. A.** (1991). Optical development of the ocular lens of an elasmobranch, *Raja eglanteria*. *Vis. Res.* **31**, 373-382.
- Smith, C. L.** (1997). *National Audubon Society field guide to tropical marine fishes of the Caribbean, the Gulf of Mexico, Florida, and the Bahamas, and Bermuda*. New York: Alfred A. Knopf.
- Smith, J. W. and Merriner, J. V.** (1985). Food habits and feeding behavior of the cownose ray, *Rhinoptera bonasus*, in lower Chesapeake Bay. *Estuaries* **8**, 305-310.
- Snelson, F. F., Jr, Williams-Hooper, S. E. and Schmid, T. H.** (1988). Reproduction and ecology of the Atlantic stingray, *Dasyatis sabina*, in Florida coastal lagoons. *Copeia* **3**, 729-739.
- Stehmann, M. and McEachran, J. D.** (1978). *FAO Species Identification Sheets for Fishery Purposes: West Atlantic, Vol. 5, Rajidae* (ed. W. Fischer). Rome: FAO.
- Watanuki, N., Kawamura, G., Kaneuchi, S. and Iwashita, T.** (2000). Role of vision in behavior, visual field, and visual acuity of cuttlefish (*Sepia esculenta*). *Fish. Sci.* **66**, 417-423.
- Young, R. F.** (1993). Observation of the mating behavior of the yellow stingray, *Urolophus jamaicensis*. *Copeia* **3**, 879-880.